



Cite this: *Chem. Sci.*, 2021, **12**, 2357

## Phosphorescent metal complexes as theranostic anticancer agents: combining imaging and therapy in a single molecule

Cai-Ping Tan, \* Yan-Mei Zhong, Liang-Nian Ji and Zong-Wan Mao \*

Phosphorescent metal complexes are a new kind of multifunctional antitumor compounds that can integrate imaging and antitumor functions in a single molecule. In this minireview, we summarize the recent research progress in this field, concentrating on the theranostic applications of phosphorescent iridium(III), ruthenium(II) and rhenium(I) complexes. The molecular design that affords these complexes with tumour- or subcellular organelle-targeting properties is elucidated. The potential of these complexes to induce and monitor the dynamic behavior of subcellular organelles and the changes in microenvironment during the process of therapy is demonstrated. Moreover, the potential and advantages of applying new technologies, such as super-resolution imaging and phosphorescence lifetime imaging, are also described. Finally, the challenges faced in the development of novel theranostic metallo-anticancer complexes for possible clinical translation are proposed.

Received 17th December 2020

Accepted 3rd January 2021

DOI: 10.1039/d0sc06885c

[rsc.li/chemical-science](http://rsc.li/chemical-science)

## 1. Introduction

At present, cancer research still faces many obstacles, such as tumour heterogeneity, drug resistance and systemic toxicity.<sup>1</sup> Although the means of cancer treatment are developing rapidly, traditional chemotherapy still plays important roles in cancer treatment.<sup>2</sup> As representatives of metallo-anticancer compounds, cisplatin and its derivatives are widely used in clinic.<sup>3</sup> In addition to platinum drugs, non-platinum metallo-anticancer agents have also attracted extensive attention, among which phosphorescent metal complexes show interesting anticancer properties due to their varied anticancer mechanisms different from that of cisplatin, as well as rich photophysical and photochemical properties that endow them with multifunctionalities.<sup>4–7</sup>

The concept “theranostics” combining “diagnosis” and “treatment” is a relatively new research trend for cancer treatment.<sup>8</sup> The original concept of “theranostics” comes from nuclear medicine. <sup>123</sup>I<sup>–</sup>, <sup>124</sup>I<sup>–</sup>, and <sup>131</sup>I with low activity are used to diagnose the disease, and <sup>131</sup>I with high activity is applied for subsequent treatment.<sup>9</sup> Now, the term is commonly used to describe multifunctional nano-platforms, in which the therapeutic and diagnostic drugs are physically combined or co-loaded on specially modified nanoparticles to integrate imaging and treatment methods.<sup>8,10</sup> Small molecules, including phosphorescent metal complexes, are also applied as “theranostic

agents” in some cases.<sup>11–13</sup> In the past few years, our group and others demonstrated that phosphorescent metal complexes can not only kill cancer cells effectively, but also provide valuable information on their action mechanisms by monitoring the cellular localization,<sup>14</sup> dynamic imaging/tracking of the subcellular organelles,<sup>15</sup> and even quantitatively measuring the parameters of the surrounding microenvironment.<sup>16</sup> Combined with super-resolution imaging,<sup>17,18</sup> two/multi-photon imaging<sup>12</sup> and phosphorescence lifetime imaging (PLIM)<sup>16</sup> technologies, more accurate and detailed information can be obtained. More importantly, these compounds have the potential to be developed as research tools for life science to accurately monitor the behaviour of subcellular organelles, functions of biomacromolecules, and changes in micro-environmental parameters (e.g., hypoxia, pH, viscosity and polarity) during various biological processes.

Recently, there have been some excellent reviews on metallo-anticancer agents published from different perspectives, such as structure–activity relationship (SAR) and anticancer mechanism analysis,<sup>19–21</sup> subcellular organelle targeting design,<sup>22</sup> bifunctionality (imaging and therapy)<sup>23</sup> and functionalization with nanomaterials.<sup>4,24</sup> This review summarizes the advantages and recent research progress in phosphorescent metal complexes as theranostic anticancer agents. The review is focused on the description of Ir(III), Ru(II) and Re(I) complexes integrating imaging and anticancer functions. We also try to clarify the challenges and possible solutions for further clinical translation of these compounds under the background of rapid development of the knowledge on cancer biology as well as fluorescence imaging techniques.

MOE Key Laboratory of Bioinorganic and Synthetic Chemistry, School of Chemistry, Sun Yat-Sen University, Guangzhou, 510275, China. E-mail: [tancaip@mail.sysu.edu.cn](mailto:tancaip@mail.sysu.edu.cn); [cesmzw@mail.sysu.edu.cn](mailto:cesmzw@mail.sysu.edu.cn)



## 2. Theranostic applications of iridium complexes

Among the iridium complexes investigated for biological applications, cyclometalated Ir(III) complexes are particularly intriguing due to their favourable photophysical properties, *e.g.*, high stability under ambient conditions, tunable emission colours, high emission quantum yields, large Stokes shifts, resistance to photobleaching and long emission lifetime.<sup>25,26</sup>

Lo's group has done a lot of research on the applications of emissive cyclometalated iridium complexes as biological molecular recognition probes, protein labelling agents, bio-orthogonal reaction reagents, bioimaging agents and photodynamic therapeutic agents.<sup>27-30</sup> They have carried out a variety of targeted modifications on iridium complexes and summarized some important factors that may influence the cellular uptake and localization of these complexes.<sup>25</sup> Li's group has also made pilot studies on iridium complexes as cellular imaging agents, particularly for complexes that can form covalent binding with biomolecules.<sup>31-33</sup> However, in these early studies, little attention has been paid on their cytotoxic mechanisms, even in some cases, they are highly cytotoxic.<sup>34</sup>

Recently, the anticancer potential of organometallic iridium complexes has been intensively explored.<sup>26</sup> Different from platinum-based drugs, iridium complexes reported mainly act by damaging different subcellular organelles.<sup>7,12,16,35</sup> Although a few reports have shown that these complexes can target the protein or DNA in cells, no definite SAR has been reported.<sup>14,36,37</sup> Iridium complexes are the most prominent ones among the metal complexes reported as theranostic anticancer agents. The cellular uptake of many drugs is usually related to their lipophilicity, while the dependence of cell penetration capabilities of iridium complexes on lipophilicity is not so obvious, and their cellular uptake mechanisms and intracellular transport pathways are largely unknown.<sup>26</sup> In many cases, phosphorescent iridium complexes show an instinct to localize to mitochondria;<sup>22</sup> however, through structural modifications, iridium complexes can also target other subcellular organelles, *e.g.*, lysosome,<sup>15</sup> lipid droplet<sup>38</sup> and endoplasmic reticulum (ER).<sup>14</sup> As the emission properties of iridium complexes are affected by the surrounding microenvironment, *e.g.*, pH<sup>39</sup> and viscosity,<sup>16</sup> they can be used to monitor the changes in these parameters in real-time.

### 2.1 Mitochondria-targeting iridium complexes

Mitochondria are the centre of energy and material metabolism in cells, and mitochondrial DNA (mtDNA) and many proteins are potential anticancer targets.<sup>40</sup> Due to the high lipophilicity and positive charge of iridium complexes, they can easily aggregate in mitochondria.<sup>22</sup> Fluorescence microscopy combined with flow cytometry and inductively coupled plasma mass spectrometry (ICP-MS) can provide valuable information on their cellular uptake levels, localization and membrane penetration mechanisms. Interestingly, mitochondria-targeting iridium complexes induce different types of cell death and varied forms of alterations in mitochondrial morphology, which

implies that they may target different biomolecules.<sup>16,41-43</sup> Recent studies have given some hints in this regard, but the clear mechanisms and SARs are still not clear.<sup>37</sup>

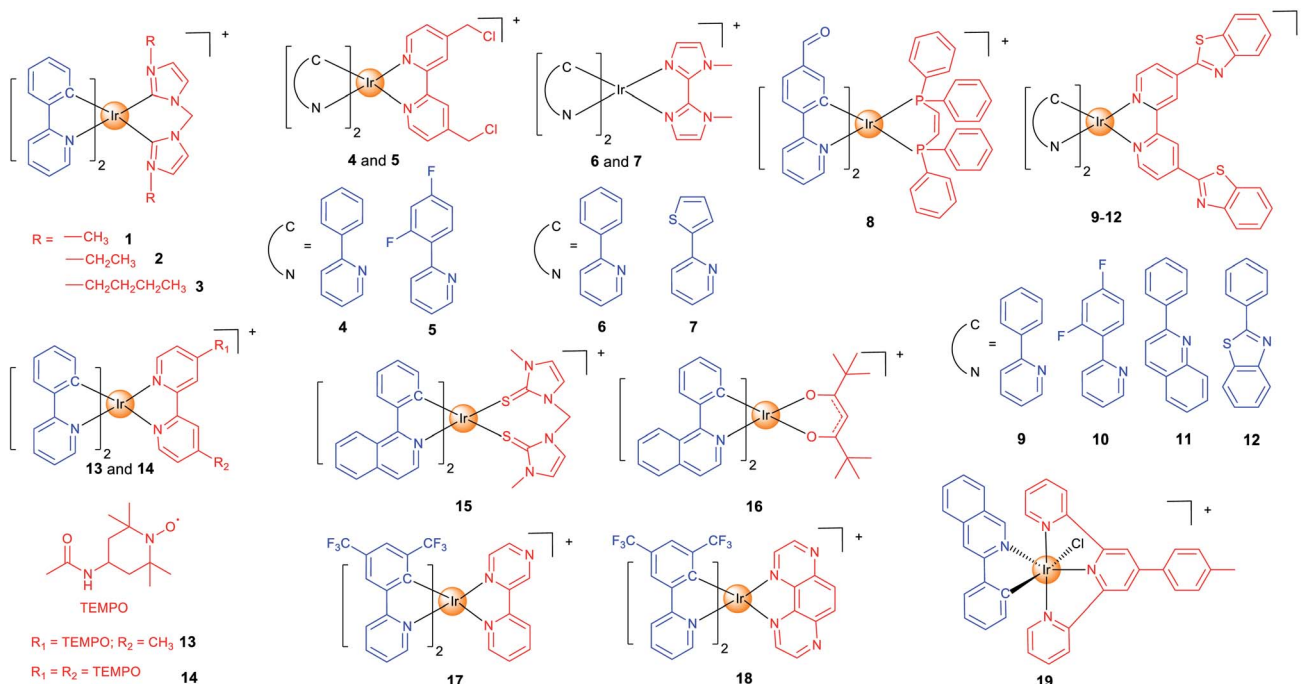
In our earlier studies, we developed a series of cyclometalated Ir(III) complexes containing different bis-N-heterocyclic carbene (NHC) ligands (1-3; Scheme 1) as photodynamic and theranostic anticancer agents.<sup>42</sup> 1-3 can quickly penetrate into human cervical carcinoma (HeLa) cells through energy-dependent pathways. The cytotoxicity of 1-3 is correlated with their lipophilicity and cellular uptake efficiency, and all of them display a higher anti-proliferative activity than cisplatin. Confocal microscopy shows that 1-3 localize in mitochondria and induce apoptosis by inducing mitochondrial damage, reactive oxygen species (ROS) production, cytochrome c release and activation of caspases. As a result, 1-3 can induce and monitor the changes in mitochondrial morphology in a real-time manner. Moreover, a very high photocytotoxicity index (PI) up to 3488 is obtained for 3 in cisplatin-resistant human lung adenocarcinoma (A549R) cells.

Aiming to increase the retention time of the complexes in mitochondria, we designed two cyclometalated Ir(III) complexes (4 and 5; Scheme 1) containing reactive chloromethyl groups that can react with thiols in mitochondrial proteins.<sup>44</sup> The immobilization of 4 and 5 on mitochondria results in an increased cellular penetration capability and cytotoxicity. Genome-wide transcriptional analysis shows that 4 exerts its anticancer activity through metabolism repression and attenuation of multiple cell death signalling pathways. Moreover, 4 causes a collapse of the normal tubular mitochondrial network into mitochondrial aggregates and large perinuclear clusters (a phenomenon observed during mitophagy), which has been subsequently confirmed by transmission electron microscopy.

Specific inducers and imaging agents of mitophagy are rarely reported. Usually, the inducer and imaging agent need to be used at the same time or in sequence to monitor a biological process. Using a single agent that can induce and monitor the biological processes simultaneously can avoid the interference of different reagents and greatly simplify the operation procedures. We identified two phosphorescent Ir(III) complexes (6 and 7; Scheme 1) that can induce and monitor the mitochondrial morphology during mitophagy.<sup>45</sup> 6 can be used to study important mitochondria-related events during mitophagy, *e.g.*, autophagosomes engulfment of mitochondria and fusion of mitochondria-engulfed autophagosomes with lysosomes.

The functional integrity of subcellular organelles is correlated with their physical parameters, *e.g.*, viscosity. However, precise quantitative measurement of viscosity at the subcellular level presents great challenges. We designed six Ir(III) complexes as mitochondrial targeting theranostic anticancer agents with viscosity-responsive phosphorescence properties.<sup>16</sup> Due to the rotatable aldehyde groups on the cyclometallating ligands and the aromatic rings on diphosphine ligands, 8 (Scheme 1) displays viscosity-dependent phosphorescence intensities and lifetimes. 8 can quantitatively monitor the self-induced changes in mitochondrial viscosity using two-photon phosphorescence lifetime imaging microscopy (TPPLIM). An obvious increase in the emission intensity/lifetime of 8 that reflects an increase in





Scheme 1 Chemical structures of mitochondria-targeting Ir(III) complexes.

mitochondrial viscosity can be observed along with the incubation time.

Oncosis is a non-apoptotic form of programmed cell death, and oncosis-inducing agents may overcome drug-resistance of the current well-established treatment regimens including platinum-based chemotherapy. Chao *et al.* presented four mitochondria-targeting cyclometalated Ir(III) complexes that could induce oncosis in drug-resistant cancer cells.<sup>35</sup> 9–12 (Scheme 1) exhibit up to ~30 times selectivity towards cancer cells over normal cells. The localization of the complexes in mitochondria was observed by confocal microscopy and verified by ICP-MS.

As stable free radicals, nitroxides have antioxidant properties mimicking superoxide dismutase and catalase, and they are widely used as spin labelling agents. Sadler *et al.* reported two luminescent Ir(III) complexes, containing one or two TEMPO (2,2,6,6-tetramethylpiperidine-1-oxyl) spin labels (13 and 14; Scheme 1).<sup>46</sup> Confocal microscopy shows that 13 and 14 localize in mitochondria. The antiproliferative activity of 14 is *ca.* 2–30× higher than that of 13 in all the cell lines tested, which may be attributed to the strong spin–spin exchange interaction between two nitroxide radicals and their conformational flexibility. Interestingly, unlike most of the other anticancer Ir(III) complexes reported, 13 and 14 with antioxidant properties show no impact on cellular ROS levels.

At present, most of the anticancer iridium complexes are not designed to target a specific biomolecule in cells. Therefore, the validation of their targets is very important to elucidate the mechanisms of action. Sadler *et al.* reported two Ir(III) complexes (15 and 16; Scheme 1) with photodynamic therapy (PDT) activities and large two-photon absorption (TPA)

properties.<sup>37</sup> PLIM experiment shows that the lifetimes of 15 and 16 inside the cells were increased by about 19-fold, which implies that the complexes reside in a more hydrophobic and hypoxic environment that are favourable for efficient photo-sensitized generation of  ${}^1\text{O}_2$ . By using the proteomic analysis, the authors demonstrated that 16 can selectively oxidize the histidines in proteins including heat shock protein 70 and aldose reductase.

PDT can mainly function through two pathways: type I process occurs through a photo-induced electron transfer to the biological substrates to form radical species including superoxide ( $\text{O}_2^{\cdot-}$ ), hydroxyl ( $\text{OH}^{\cdot}$ ), and hydroperoxyl ( $\text{HO}_2^{\cdot}$ ); type II process generates singlet oxygen ( ${}^1\text{O}_2$ ) by a direct energy transfer to  $\text{O}_2$ . Most photosensitizers (PSs) act through type II process that requires the participation of  $\text{O}_2$ . Unfortunately, tumour microenvironment (TME) is hypoxic. Elias *et al.* developed two Ir(III) complexes (17 and 18; Scheme 1) that can exert their PDT effects through type I process independent of  $\text{O}_2$ .<sup>47</sup> 17 and 18 accumulate in mitochondria in the 2D cell monolayer, and both complexes are evenly distributed on slices of 3D multicellular tumour spheroids (MCTSs). However, 17 is more dependent on type II PDT, while type I plays a greater role in 18-mediated photo-initiated cell death, so 18 displays a better PDT effect in MCTSs simulating the hypoxic TME.

Also to overcome the hypoxic TME, Sadler *et al.* resorted to another strategy.<sup>48</sup> Complex 19 (Scheme 1) can catalytically oxidize 1,4-dihydronicotinamide adenine dinucleotide (NADH) to generate  $\text{NAD}^{\cdot}$  radicals under light irradiation. Moreover, it perturbs the electron transfer pathways in mitochondria by reducing  $\text{Fe}^{3+}$ -cytochrome c, which breaks the redox imbalance in cancer cells. As these photoredox catalyzing reactions are  $\text{O}_2^{\cdot-}$



independent, **19** is equipotent towards normoxic and hypoxic adherent cancer cells. Confocal microscopy shows that **19** is localized in mitochondria, and it can induce immunogenic apoptotic cell death upon irradiation with a two-photon light source.

## 2.2 Lysosome-targeting iridium complexes

Lysosomes contain hydrolytic enzymes that can degrade macromolecules for turnover of the nutrients.<sup>49</sup> In addition, lysosomes also participate in regulation of different types of cell death, *e.g.*, apoptosis and autophagy. Especially, lysosomal trafficking and contents are important factors that regulate autophagy.<sup>50</sup> Our group developed two iridium(III) complexes (**20** and **21**; Scheme 2) as one- and two-photon-excited theranostic agents for real-time tracking of autophagic lysosomes.<sup>12</sup> The protonation/deprotonation of secondary amines in indole rings on the  $\beta$ -carboline ligands results in the pH-sensitive phosphorescence properties of **20** and **21**. The  $pK_a$  values of **20** and **21** are 5.56 and 5.19, respectively, which are very close to the lysosomal pH. By combining selective autophagy-inducing and lysosomal imaging capabilities in a single molecule, **21** can track the key events during autophagy including autophagosomal-lysosomal fusion in live cells in a real-time manner.

The whole process of autophagy, called “autophagic flux”, includes the formation and maturation of autophagosomes, fusion of autophagosomes with lysosomes, the degradation of the cargoes and the release of the degradation products. Based on the previous work,<sup>12</sup> we reported two Ir(III) complexes with 2,2'-biimidazole ( $H_2$ biim, **22**) or 2-(1H-imidazol-2-yl)pyridine (Hpyim, **23**) as the ancillary ligands (Scheme 2). **22** and **23** are kinetically stable, and no trace of decomposition is observed in human plasma for 72 h. **22** and **23** can image lysosomes as they display pH-dependent phosphorescence caused by the protonation and deprotonation process of the N-H groups on  $H_2$ biim/Hpyim. Interestingly, both **22** and **23** can act as anion transporters to inhibit autophagic flux by alkalinizing lysosomes.<sup>51</sup>

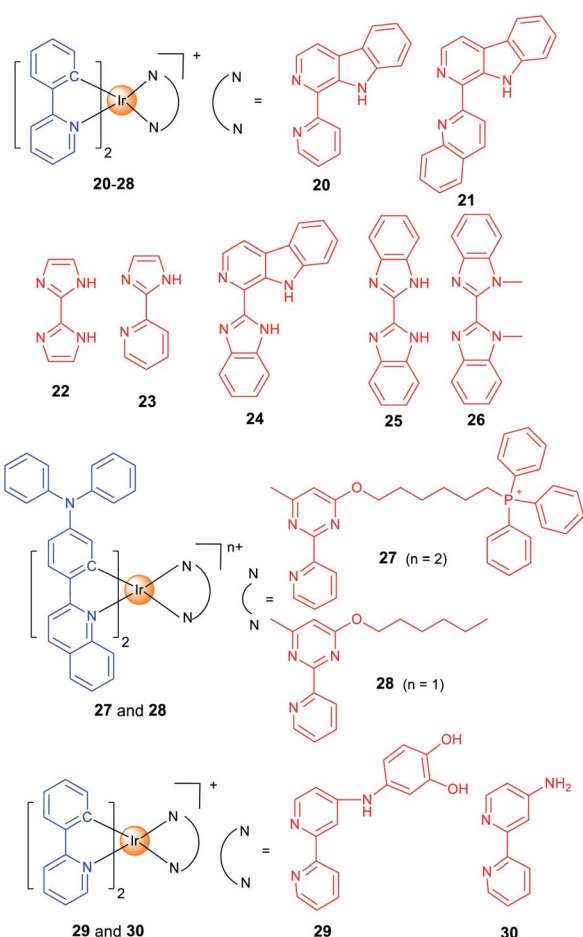
By structural optimization, we developed a series of Ir(III) complexes as stimuli-activatable PSs targeting lysosomes.<sup>15</sup> Complex **24** (Scheme 2) shows enhanced phosphorescence emission and  $^1O_2$  generation in tumour/lysosome-related acidic environments ( $pH \leq 6.5$ ) and exhibits a high photocytotoxicity ( $PI > 833$ ) in human lung adenocarcinoma (A549) cells upon visible light exposure. **24** can photodamage and image lysosomes simultaneously, which provides a reliable and convenient method for real-time monitoring of the outcome of treatment. Later, we designed four cyclometalated Ir(III) complexes containing benzimidazole derivatives as ancillary ligands which exhibit dual anticancer functionalities as effective PSs and metastasis inhibitors.<sup>52</sup>

Most of the metal complexes applied for PDT utilize UV/Vis light with limited penetration depth; two-photon excitation (TPE) that simultaneously absorbs two lower-energy NIR (near-infrared)-photons can overcome this shortage. Weinstein and Bryant *et al.* reported two photo-stable Ir(III) complexes (**25** and **26**) with long-lived triplet excited states as photosensitizers that can be excited under both one- and two-photon light.<sup>53</sup>

Both **25** and **26** are cell-permeable, and **26** shows higher dark cytotoxicity while **25** possesses more potent PDT activity (lowest  $PI$  value  $>333$ ). **25** localizes in mitochondria and lysosomes sequentially alone with the incubation time, and it can disrupt the functions of both organelles to induce apoptosis upon light irradiation. More importantly, **25** maintains high PDT activity under NIR TPE (760 nm) at low concentrations and light doses.

Targeting different subcellular organelles can achieve different antitumor effects and mechanisms. For example, Huang and Zhao *et al.* designed two Ir(III) complexes with different substituent groups on the ancillary ligand (**27** and **28**; Scheme 2).<sup>54</sup> Interestingly, HeLa cells treated with the mitochondria-targeting **27** maintains a slower  $O_2$  consumption rate and higher intracellular  $O_2$  level under hypoxia. So, **27** exhibits an improved PDT effect as compared with the lysosome-targeting **28** under hypoxia.

Some complexes can even change the subcellular localization through chemical reactions and exert their antitumor effect through a sequential localization process. Chao *et al.* reported a prodrug **29** (Scheme 2) that is firstly localized in lysosomes and subsequently transferred to mitochondria.<sup>55</sup> The meta-imino catechol group in **29** can be oxidized by  $Fe^{3+}$  inside the cell to release  $Fe^{2+}$ , the aminobipyridyl complex **30** and 2-hydroxybenzoquinone.  $Fe^{2+}$  can transform  $H_2O_2$  into  $^{\bullet}OH$



Scheme 2 Chemical structures of lysosome-targeting Ir(III) complexes.



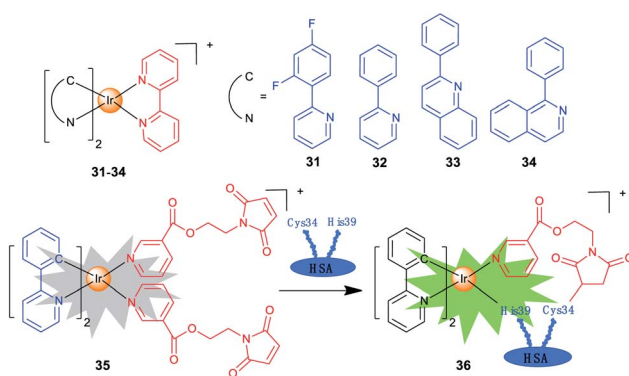
through the Fenton reaction, and the benzoquinone compound can interfere with the respiratory chain. Interestingly, the transformation of **29** into **30** leads to an increase in phosphorescence/cytotoxicity, and the migration of subcellular localization from lysosome to mitochondria can be tracked by confocal microscopy.

### 2.3 Iridium complexes targeting other organelles

Iridium complexes with theranostic functions can also localize in other subcellular organelles, such as ER and nuclei through structural modifications. Lim *et al.* investigated the PDT mechanisms of four Ir(III) complexes (**31–34**; Scheme 3) containing different cyclometallating ligands.<sup>14</sup> The most active complex **33** is primarily localized in ER and partially in mitochondria. The localization of **33** is also confirmed by lifetime imaging that shows an extended emission lifetime (*ca.* 500 ns) in the vicinity of ER. Interestingly, upon light irradiation, **33** prompts cell death *via* photo-cross-linking of proteins, and oxidation of several essential proteins (*e.g.*, TRAP1 and PYCR1) in ER and mitochondria. Moreover, **33** exhibits TPA properties, making them ideal candidates for effective PDT with deep-tissue imaging capabilities.

Che *et al.* reported a panel of luminescent Ir(III) porphyrin complexes containing axial NHC ligands.<sup>56</sup> The IC<sub>50</sub> values obtained for these complexes are in the nanomolar levels upon light irradiation. Confocal microscopy shows that the most active compound acts by targeting ER and catalysing the generation of <sup>1</sup>O<sub>2</sub> to trigger protein oxidation and apoptosis.

One of the biggest obstacles for the application of iridium complexes in cancer treatment is the lack of selectivity for cancer cells. Human serum albumin (HSA) is an effective, nontoxic, biocompatible and biodegradable drug delivery vehicle. Sadler *et al.* designed a maleimide-functionalized Ir(III) complex **35** (Scheme 3) that could react with HSA to form a conjugate **36** for PDT.<sup>57</sup> The conjugation to HSA greatly enhances the phosphorescence and <sup>1</sup>O<sub>2</sub> sensitization capability of **35**, and the as-formed **36** accumulates mostly in the nuclei of cancer cells. Both **35** and **36** are encouragingly nontoxic toward normal cells, and a high photocytotoxicity (PI = 56.6) is obtained for **36** upon irradiation.



Scheme 3 Chemical structures of Ir(III) complexes targeting other subcellular organelles.

## 3. Theranostic applications of ruthenium complexes

Ruthenium-based anticancer agents have many intriguing properties, which include good selectivity towards tumour cells, suitable ligand exchange kinetics, and variable biologically accessible oxidation states. Four ruthenium complexes have entered different stages of clinical trials, including **NAMI-A**, **KP1019**, **NKP-1339** and **TLD1433**.<sup>4,20,58</sup> On the other hand, Ru(II) polypyridyl complexes are the most extensively studied and developed systems among the ruthenium complexes with bio-imaging and biosensing applications.<sup>59</sup>

The biological application of luminescent ruthenium complexes originated from the pioneer work done by Barton *et al.* They found that these molecules could be used as molecular light switches for DNA, and had the ability to distinguish different DNA structures.<sup>60,61</sup> In 2007, they first used fluorescence microscopy to study the cellular uptake properties of Ru(II) polypyridyl complexes.<sup>62</sup> Since then, the bioimaging and anticancer potential of luminescent polypyridyl ruthenium complexes has been gradually explored.

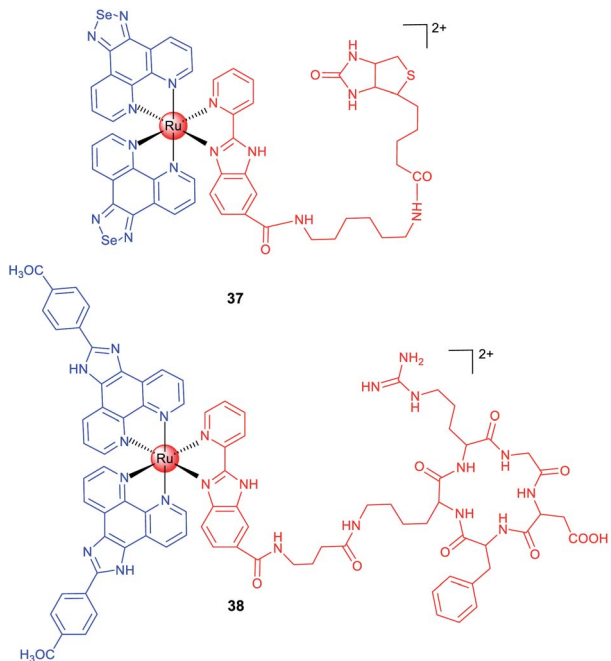
Ru(II) polypyridyl complexes are known to possess metal-to-ligand charge transfer red emission, large Stokes shift, long emission lifetimes and two/multi-photon absorption properties.<sup>21</sup> Due to the phosphorescence quenching effect caused by the energy transfer between the triplet excited state of Ru(II) complexes and the triplet ground state of O<sub>2</sub>, the luminescence properties of ruthenium complexes are sensitive to O<sub>2</sub>, and they are used as commercial O<sub>2</sub> probes.<sup>63</sup> Moreover, Ru(II) polypyridyl complexes can target different subcellular organelles for super-resolution imaging, *e.g.*, stimulated emission depletion imaging.<sup>64,65</sup>

Although selectivity towards cancer cells and subcellular organelle-targeting properties can be achieved through structural optimizations, *e.g.*, modulation of the molecular charge and lipophilicity, sometimes these strategies turn out to be unsuccessful. In several cases, the conjugation of the Ru(II) polypyridyl moiety with biological vectors, such as tumour-specific recognition groups and subcellular organelle-targeting peptides, has been proved to be very effective.<sup>66–68</sup> The intrinsic phosphorescence properties of the complexes can be used to verify the original structural design using fluorescence imaging technologies both *in vivo* and *in vitro*.

Biotin is an efficient tumour-targeting ligand that can bind to its surface receptors overexpressed in tumour cells. Chen *et al.* reported a biotin-modified Ru(II) complex (**37**; Scheme 4) that can be preferentially ingested by HeLa cells through a receptor-mediated endocytosis pathway for imaging of cancer cells both *in vitro* and *in vivo*.<sup>66</sup> A similar strategy was adopted by Chao *et al.*, and they designed a biotin-modified Ru(II)-based PS with cancer cell targeting ability in an *in vitro* co-cultured model (mixed cultivation of A549R and human lung fibroblast (HLF) cells).<sup>67</sup>

In the past few decades, scientists have discovered a variety of peptides to recognize cancer cells, different subcellular organelles and protein targets. Chen *et al.* conjugated a cRGD





**Scheme 4** Chemical structures of ruthenium complexes with targeting groups.

peptide with a Ru(II) moiety (38; Scheme 4) for selective targeting of integrin-overexpressed cancer cells.<sup>68</sup> 38 preferentially accumulates at the tumour sites in xenograft mice after intravenous injection and effectively inhibits tumour growth without causing pathological tissue damage or abnormalities. Encouragingly, 38 shows potential for precise tumour diagnosis and therapy *in vivo*, and exhibits distinct binding capabilities for different grades of cervical carcinoma specimens from clinical patients, supporting its potential applications in rapid tumour diagnosis.

### 3.1 Subcellular organelle-targeting ruthenium complexes

There are several strategies to optimize the anticancer and imaging performance of ruthenium complexes. Some Ru(II) complexes have instinct subcellular targeting properties, and many Ru(II) complexes tend to accumulate in mitochondria.<sup>19</sup> Active targeting can be achieved by structural decoration, such as conjugation with moieties targeting a certain protein, nucleic acids or subcellular organelles.<sup>21</sup>

In many cases, fluorescence imaging technology is used to elucidate the action mechanisms of these complexes. Chao *et al.* designed a series of Ru(II) polypyridyl complexes containing a ligand with the triphenylphosphine substituent that is widely used as the mitochondrial targeting group.<sup>69</sup> As expected, 39 (Scheme 5) localizes in mitochondria and exhibits a 28-fold enhancement in cytotoxicity when exposed to a low dose of visible light in HeLa cells.

Peptide-based vectors are also used to modify Ru(II) complexes to endow them with capabilities to target subcellular organelles. Keyes *et al.* constructed a Ru-dppz complex conjugated with a nuclear localization signal peptide sequence (40;

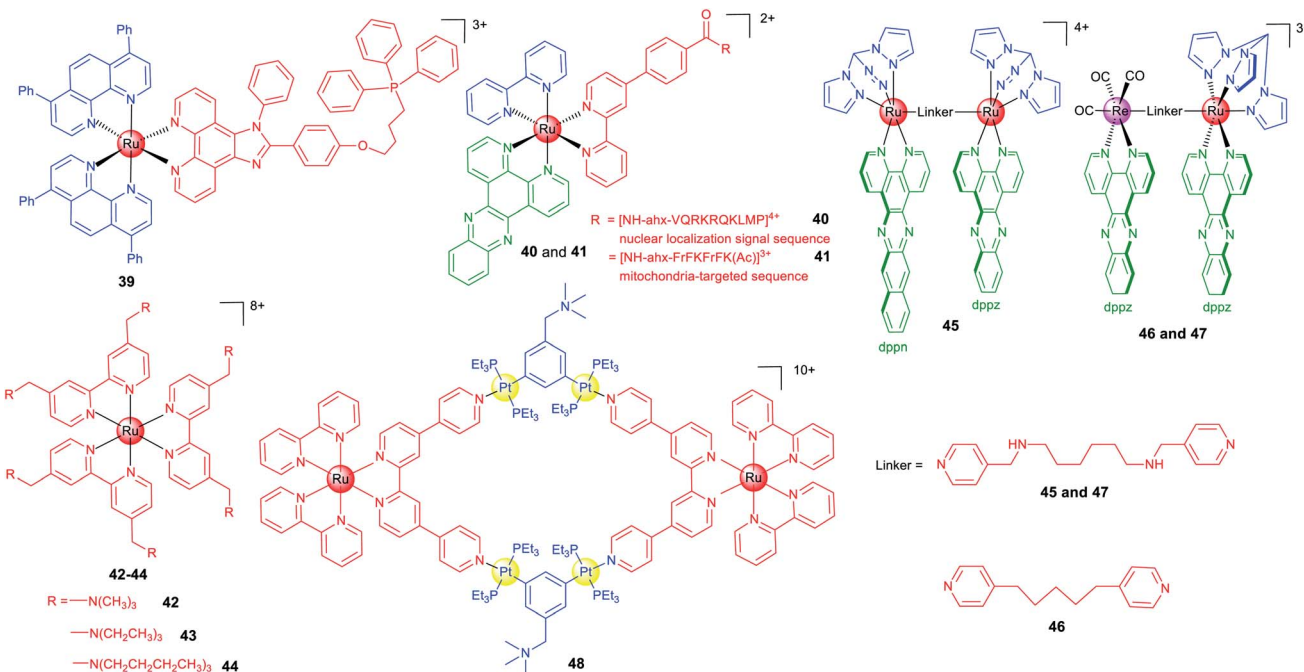
Scheme 5) to direct the complex to the nuclei of HeLa cells successfully.<sup>64</sup> Later, they reported a mitochondria-targeting molecular light switch (41; Scheme 5) by peptide vectorization, considering that mtDNA plays crucial roles in cancer.<sup>70</sup> By using techniques including confocal fluorescence microscopy, Raman imaging, and luminescence lifetime imaging, they demonstrated that 41 could bind to and image mtDNA. Moreover, in the presence of intense irradiation, 41 can effectively stimulate cell death.

Lysosome may be a more suitable targeting subcellular organelle for PDT, as targeting the mitochondrion can result in high dark cytotoxicity, while targeting the nucleus can easily cause gene mutation. Based on these considerations, Chao *et al.* reported three highly charged Ru(II) polypyridyl complexes (42–44; Scheme 5) that could accumulate in lysosomes through endocytosis and are basically nontoxic in the dark.<sup>71</sup> Upon two-photon light irradiation, 42–44 show impressive photocytotoxicity in both monolayers and MCTSs. Mechanism investigation shows that 42–44 cause oxidative stress in cells in the presence of light irradiation and induce cell death by necrosis.

Generally, ruthenium complexes containing planar ligands can bind to DNA tightly under physiological conditions. Imaging technology provides clues for target validation of these compounds, which shows that nuclear DNA may not be their primary targets. Thomas *et al.* designed one mononuclear and three dinuclear complexes with either homoleptic or heteroleptic structures.<sup>72</sup> The Ru(II) dppz units usually exhibit a “DNA light switch” effect, while dppn-based complexes commonly have a long lifetime based on the  $\pi \rightarrow \pi^*$  excited state favourable for  $^1\text{O}_2$  sensitization. Although complex 45 (Scheme 5) binds to DNA under cell-free conditions, confocal microscopy shows that it localizes in mitochondria and especially lysosomes, which implies damaging nuclear DNA may not be involved in its PDT mechanism. Recently, the same group reported two dinuclear complexes (46 and 47; Scheme 5) containing the Ru(II)-dppz and Re(I)-dppz moieties with different linking ligands.<sup>18</sup> Steady-state and time-resolved photophysical studies reveal that the nature of the linkers affects the excited state dynamics of 46 and 47 and their DNA photo-cleavage properties. Their intracellular localizations and photocytotoxicity are significantly affected by the linkers. Notably, 47 initially localizes in mitochondria and lysosomes of live cells, while strong staining of the nucleus and particularly the nuclear membrane can be observed within 5 min.

The coupling of polymeric compounds can also improve the optical properties and anticancer effects as compared with the mono-nuclear compounds. Based on a Ru(II) polypyridyl donor and a tetramethylammonium-decorated Pt(II) acceptor, Stang and Chao *et al.* reported a heterometallic Ru–Pt metallocycle (48; Scheme 5) *via* coordination-driven self-assembly.<sup>73</sup> The rigid, planar macrocyclic structure of 48 enhances the favourable photophysical properties including red-shifted emission, enhanced TPA activities and improved intersystem crossing for more efficient ROS generation upon irradiation. Moreover, the highly charged hydrophobic bis(phosphine) Pt(II) building block facilitates the cellular uptake efficiency, and





Scheme 5 Chemical structures of Ru(II) complexes targeting subcellular organelles.

confocal microscopy shows that **48** localizes in both mitochondria and nuclei.

#### 4. Theranostic applications of rhenium complexes

Radioactive  $^{186/188}\text{Re}$  has been used in clinical treatment of cancer, and the “cold” organometallic rhenium complexes are mainly used as cell imaging reagents and photocatalysts.<sup>25</sup> The most common structural motif applied in biological systems is the stable Re(I) tricarbonyl core, and its facile synthesis can be used to generate a wide range of compounds the properties of which can be tuned to maximize biological activity.<sup>6</sup> Recently, more and more studies have shown that organometallic rhenium complexes have potent anticancer activity. Coupled with their excellent phosphorescence properties, the cellular distribution and localization can be monitored by fluorescence microscopy and lifetime imaging.<sup>74</sup> Lo’s group studied the emissive properties of rhenium complexes and their potential as biological probes, bioorthogonal reaction reagents, cellular imaging agents and anticancer photosensitizers.<sup>75-78</sup> Metzler Nolte *et al.* focused on the conjugation of these complexes with biomolecules and their anticancer activities as well as cytotoxic mechanisms.<sup>79,80</sup>

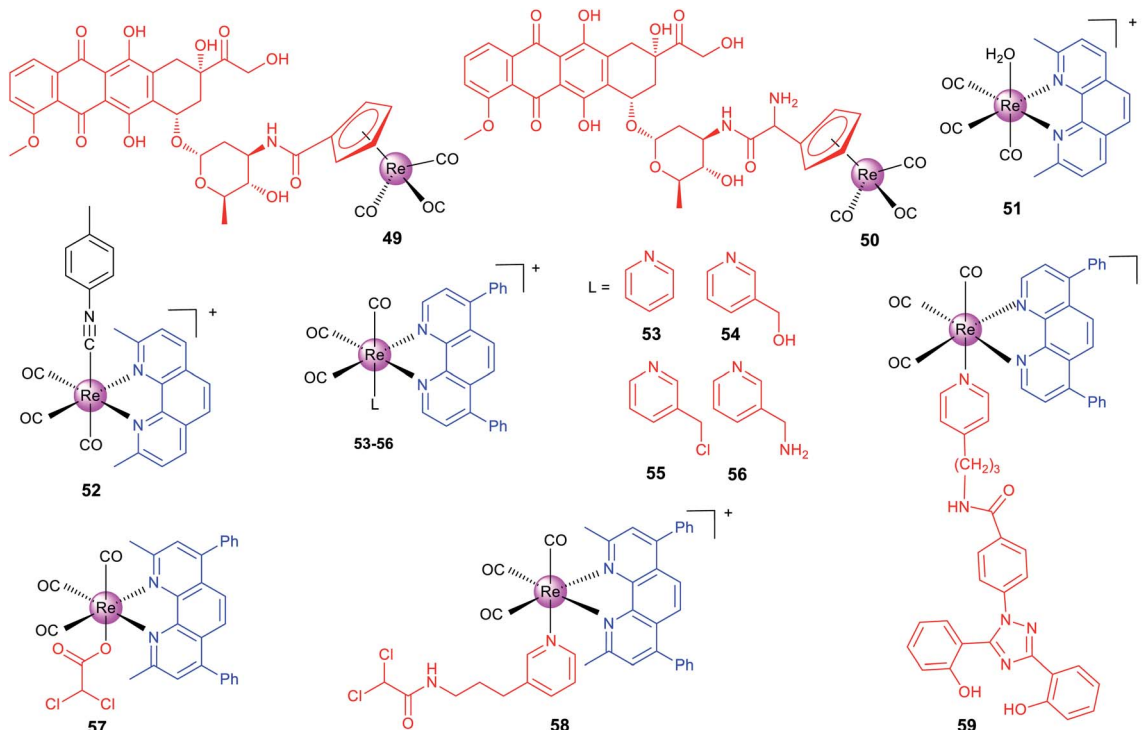
The  $[\text{Re}(\text{CO})_3]^+$  core can be easily synthesized and modified with functional groups or targeting moieties, and they can also be used for vibrational imaging. The same set of ligands of  $[\text{Re}(\text{CO})_3]^+$  can be coordinated to the  $[\text{^{99m}Tc}(\text{CO})_3]^+$  core to synthesize the corresponding radioimaging reagents and radiopharmaceuticals, which offers another opportunity for their *in vivo* applications.<sup>81</sup> Another intriguing possibility is that

Re(I) tricarbonyl complexes may deliver CO to the targeted sites and act as photoactivatable CO-releasing molecules.<sup>82</sup> Although a considerable number of rhenium complexes have been reported as potent anticancer agents until now, the mechanisms of their cytotoxic effect are barely elucidated.

Alberto *et al.* reported two organometallic complexes (**49** and **50**; Scheme 6) formed by the conjugation of the rhenium cyclopentadienyl moiety with doxorubicin (DOX; a topoisomerase II inhibitor).<sup>83</sup> Interestingly, the conjugation redirects DOX from the nuclei to mitochondria. Confocal microscopy shows that **49** localizes to mitochondria. ICP-MS also proves that most of the total internalized rhenium of **49** and **50** accumulates in the nuclei (~60%), and about 20–30% is found in mitochondria. Accordingly, **49** and **50** exert their anticancer effects by disrupting the mitochondrial membrane potential and inhibiting human topoisomerase II simultaneously. It should be pointed out that the emission used for confocal imaging originates from the DOX chromophore rather than the metal center.

Recently, Wilson’s group has made a series of efforts to reveal the SARs, stability and mechanisms of rhenium complexes.<sup>81,84-87</sup> The distribution and metabolism of drugs *in vivo* are very important issues for their potential clinical applications. However, few non-platinum-based metallo-anticancer agents have been studied in this aspect. Wilson *et al.* reported seven Re(I) complexes of the general formula  $\text{fac-}[\text{Re}(\text{CO})_3(\text{N-N})(\text{OH}_2)]^+$ , where N-N represents different bidentate ligands.<sup>81</sup> Confocal microscopy indicates that the most active complex (**51**, Scheme 6) accumulates in some populations of endosomes and lysosomes. Semi-quantitative measurement using flow cytometry shows that **51** penetrates into cancer cells through the endocytotic pathway. Interestingly, **51** acts through a novel mode of action by inducing a non-canonical cell death that





Scheme 6 Chemical structures of theranostic Re(I) complexes.

cannot be categorized as apoptosis, necrosis, paraptosis, or autophagy.

Importantly, the authors also prepared the  $^{99m}\text{Tc}$  analogue for *in vivo* imaging and biodistribution studies, and they found that both 51 and its  $^{99m}\text{Tc}$  analogue were excreted by the hepatobiliary system. Interestingly, they subsequently used ICP-MS to find that 51 shows similar uptake in both cisplatin-sensitive and -resistant cell lines, and 51 tends to concentrate in mitochondria.<sup>84</sup> This result is different from that observed by fluorescence microscopy, because the emission of 51 depends on the pH and coordination environment. At the same time, they also proved that 51 is effective on patient derived ovarian cancer tumour xenografts, which further proves its potential as an anticancer candidate.

Wilson *et al.* also developed another rhenium(I) tricarbonyl complex (52) containing a chelating polypyridyl ligand and an axial isonitrile ligand as an anticancer candidate.<sup>87</sup> 52 is stable for at least one week in the solid state and aqueous solutions. Moreover, X-ray fluorescence microscopy shows that 52 is highly stable *in vitro*.<sup>86</sup> 52 shows strong anticancer activity on a variety of cell lines *in vitro* and can inhibit A2780 ovarian cancer xenografts and prolong mouse survival *in vivo*. 52 shows partial colocalization with the LysoTracker Red dye and GalT-dsRed fusion protein.<sup>87</sup> It triggers unfolded protein response, ER stress, autophagy and apoptotic cell death. Similar *in vivo* bio-distribution patterns were observed for 52 and its  $^{99m}\text{Tc}$  congener, which suggests that the  $^{99m}\text{Tc}$  analogue can be used as its diagnostic partner. Later, the authors constructed a 52-resistant ovarian cancer cell line, and identified two genes (the ATP-binding cassette transporter P-glycoprotein and MT1

encoding metallothioneins) involved in its resistance responses.<sup>85</sup>

Targeting cancer metabolism and reversing its metabolic machine have emerged as promising strategies for cancer therapy. Our group designed a series of phosphorescent Re(I) complexes (53–56; Scheme 6) with a highly lipophilic bidentate ligand as mitochondria-targeting theranostic anticancer agents.<sup>74</sup> 53–56 can quickly and efficiently penetrate into A549 cells and localize in mitochondria. Notably, 55, containing a thiol-reactive chloromethylpyridyl moiety, can be immobilized in mitochondria and induce a cascade of mitochondria-dependent apoptotic events. The  $\text{O}_2$ -sensitive lifetimes of 55 are utilized to track the self-induced mitochondrial respiration repression using PLIM in a real-time manner. Based on this work, our group also synthesized two theranostic Re-DCA (DCA; dichloroacetate; a pyruvatedehydrogenase kinase inhibitor) conjugates (57 and 58; Scheme 6) that can selectively accumulate in mitochondria to reverse the cancer cell metabolism from glycolysis to glucose oxidation.<sup>88</sup>

Mitochondria are the main sites for ROS production, and glutathione (GSH) in mitochondria is critical for ROS scavenging through GSH reductase and peroxidase systems. Aiming to break the GSH metabolism and redox homeostasis in cancer cells, our group synthesized two mitochondria-accumulating binuclear Re(I) tricarbonyl complexes, in which the azo/disulfide bond in the bridge linkage group could react with GSH.<sup>89</sup> These complexes can localize in mitochondria, cause oxidative mitochondrial dysfunction, and induce necroptosis and caspase-dependent apoptosis simultaneously.



The malignancy of cancer is characterized by the changes in the epigenetic modification landscape. Recently, our group reported a mitochondria-targeting Re(1) complex **59** (Scheme 6) that could demolish triple-negative breast cancer cells by influencing their epigenetic status and inducing immunogenic apoptotic cell death.<sup>90</sup> By integrating the clinical iron chelating agent deferasirox into its structure, **59** can relocate iron to mitochondria and change the key metabolic species related to the machinery of epigenetic modifications. Confocal microscopy shows that **59** localizes in mitochondria and the emission of **59** is gradually quenched along with the incubation time, which further confirms that Fe is relocated to mitochondria because both Fe<sup>2+</sup> and Fe<sup>3+</sup> can quench the fluorescence of **59**.

## 5. Conclusions

Phosphorescent metal complexes have shown great potential as multifunctional anticancer compounds that can integrate imaging and therapeutic functionalities. On one hand, the imaging function can provide useful clues for the investigation of their anticancer mechanisms, such as their localization on the subcellular organelles. On the other hand, they can be utilized to track the dynamic behaviors of subcellular organelles during various types of cell death depending on their unique anticancer mechanisms. Of course, the research field is still in its infancy, and there are still many unresolved problems as well as room for improvement for their theranostic applications.

In future research, we propose that the following aspects are very important for the development of this field. (1) The excitation and emission wavelengths of most complexes reported are in the visible region with limited penetration depth. More structural optimization is needed to tune the optical properties of the complexes to the NIR region, which is more suitable for *in vivo* applications. The correlation between the structural design and the function of the complexes is not straightforward with many of the reports displaying certain randomness. Combined with new imaging technologies (*e.g.*, super-resolution imaging), the rational design of phosphorescent metal complexes to more accurately reflect the behaviours of subcellular organelles and biomolecules during the process of therapy is still challenging. (2) Molecular target validation of the complexes needs to be strengthened, which can help to explain their cellular behaviors and more accurately correlate with the specific biological processes monitored by their imaging function. At present, some studies have demonstrated that metallo-compounds can bind with diverse biomolecules in cells, but the biomolecular targets of many complexes in cells are unknown. (3) The mechanism of the uptake, transport, storage and metabolism of the complexes *in vitro* and *in vivo* is not clear, and the specific pathways or biomolecules responsible for these processes are unknown. The stability of the complexes under physiological conditions has been rarely investigated, and new *in situ* research methods are needed to explore their stability both in cells and *in vivo*. (4) Finally, with regard to the potential clinical transformations of these complexes, it is necessary to construct a much larger library for accurate SAR exploration. The multi-omics approach can be utilized to uncover their global

biological effects. Moreover, we should seek cooperation with experts in pharmacology, oncology, clinical research and pharmaceutical industry to explore the possibility of their clinical translation.

## Conflicts of interest

There are no conflicts to declare.

## Acknowledgements

This study was supported by the National Natural Science Foundation of China (nos. 22022707, 21778078 and 21837006), the innovative team of Ministry of Education (no. IRT\_17R111) and the Fundamental Research Funds for the Central Universities.

## Notes and references

- I. Dagogo-Jack and A. T. Shaw, *Nat. Rev. Clin. Oncol.*, 2018, **15**, 81–94.
- T. Powles, I. Duran, M. S. van der Heijden, Y. Loriot, N. J. Vogelzang, U. De Giorgi, S. Oudard, M. M. Retz, D. Castellano, A. Bamias, A. Flechon, G. Gravis, S. Hussain, T. Takano, N. Leng, E. E. Kadel 3rd, R. Banchereau, P. S. Hegde, S. Mariathasan, N. Cui, X. Shen, C. L. Derleth, M. C. Green and A. Ravaud, *Lancet*, 2018, **391**, 748–757.
- T. C. Johnstone, K. Suntharalingam and S. J. Lippard, *Chem. Rev.*, 2016, **116**, 3436–3486.
- L. L. Zeng, P. Gupta, Y. L. Chen, E. J. Wang, L. N. Ji, H. Chao and Z. S. Chen, *Chem. Soc. Rev.*, 2017, **46**, 5771–5804.
- A. Notaro and G. Gasser, *Chem. Soc. Rev.*, 2017, **46**, 7317–7337.
- L. C. C. Lee, K. K. Leung and K. K. W. Lo, *Dalton Trans.*, 2017, **46**, 16357–16380.
- D. L. Ma, C. Wu, K. J. Wu and C. H. Leung, *Molecules*, 2019, **24**, 2739.
- J. Xie, S. Lee and X. Chen, *Adv. Drug Delivery Rev.*, 2010, **62**, 1064–1079.
- L. Filippi, A. Chiaravalloti, O. Schillaci, R. Cianni and O. Bagni, *Expert Rev. Med. Devices*, 2020, **17**, 331–343.
- C. Wang, W. Fan, Z. Zhang, Y. Wen, L. Xiong and X. Chen, *Adv. Mater.*, 2019, **31**, 1904329.
- R. Kumar, W. S. Shin, K. Sunwoo, W. Y. Kim, S. Koo, S. Bhuniya and J. S. Kim, *Chem. Soc. Rev.*, 2015, **44**, 6670–6683.
- L. He, C. P. Tan, R. R. Ye, Y. Z. Zhao, Y. H. Liu, Q. Zhao, L. N. Ji and Z. W. Mao, *Angew. Chem., Int. Ed.*, 2014, **53**, 12137–12141.
- C. R. Cardoso, M. V. Lima, J. Cheleski, E. J. Peterson, T. Venancio, N. P. Farrell and R. M. Carlos, *J. Med. Chem.*, 2014, **57**, 4906–4915.
- J. S. Nam, M. G. Kang, J. Kang, S. Y. Park, S. J. C. Lee, H. T. Kim, J. K. Seo, O. H. Kwon, M. H. Lim, H. W. Rhee and T. H. Kwon, *J. Am. Chem. Soc.*, 2016, **138**, 10968–10977.
- L. He, Y. Li, C. P. Tan, R. R. Ye, M. H. Chen, J. J. Cao, L. N. Ji and Z. W. Mao, *Chem. Sci.*, 2015, **6**, 5409–5418.



16 L. Hao, Z. W. Li, D. Y. Zhang, L. He, W. Liu, J. Yang, C. P. Tan, L. N. Ji and Z. W. Mao, *Chem. Sci.*, 2019, **10**, 1285–1293.

17 Q. X. Chen, C. Z. Jin, X. T. Shao, R. L. Guan, Z. Q. Tian, C. R. Wang, F. Liu, P. X. Ling, J. L. Guan, L. N. Ji, F. S. Wang, H. Chao and J. J. Diao, *Small*, 2018, **14**, 1802166.

18 H. K. Saeed, S. Sreedharan, P. J. Jarman, S. A. Archer, S. D. Fairbanks, S. P. Foxon, A. J. Auty, D. Chekulaev, T. Keane, A. J. H. M. Meijer, J. A. Weinstein, C. G. W. Smythe, J. B. de la Serna and J. A. Thomas, *J. Am. Chem. Soc.*, 2020, **142**, 1101–1111.

19 F. Heinemann, J. Karges and G. Gasser, *Acc. Chem. Res.*, 2017, **50**, 2727–2736.

20 S. Monro, K. L. Colon, H. M. Yin, J. Roque, P. Konda, S. Gujar, R. P. Thummel, L. Lilge, C. G. Cameron and S. A. McFarland, *Chem. Rev.*, 2019, **119**, 797–828.

21 F. E. Poynton, S. A. Bright, S. Blasco, D. C. Williams, J. M. Kelly and T. Gunnlaugsson, *Chem. Soc. Rev.*, 2017, **46**, 7706–7756.

22 Y. Chen, T. W. Rees, L. N. Ji and H. Chao, *Curr. Opin. Chem. Biol.*, 2018, **43**, 51–57.

23 C. N. Ko, G. D. Li, C. H. Leung and D. L. Ma, *Coord. Chem. Rev.*, 2019, **381**, 79–103.

24 J. G. Liu, H. Q. Lai, Z. S. Xiong, B. L. Chen and T. F. Chen, *Chem. Commun.*, 2019, **55**, 9904–9914.

25 K. K. W. Lo, *Acc. Chem. Res.*, 2015, **48**, 2985–2995.

26 C. Caporale and M. Massi, *Coord. Chem. Rev.*, 2018, **363**, 71–91.

27 H. Chen, Q. Zhao, Y. Wu, F. Li, H. Yang, T. Yi and C. Huang, *Inorg. Chem.*, 2007, **46**, 11075–11081.

28 K. K. Lo, C. K. Chung and N. Zhu, *Chem.-Eur. J.*, 2006, **12**, 1500–1512.

29 K. K. Lo, C. K. Chung, T. K. Lee, L. H. Lui, K. H. Tsang and N. Zhu, *Inorg. Chem.*, 2003, **42**, 6886–6897.

30 K. K. Lo, *Acc. Chem. Res.*, 2020, **53**, 32–44.

31 C. Li, M. Yu, Y. Sun, Y. Wu, C. Huang and F. Li, *J. Am. Chem. Soc.*, 2011, **133**, 11231–11239.

32 M. Yu, Q. Zhao, L. Shi, F. Li, Z. Zhou, H. Yang, T. Yi and C. Huang, *Chem. Commun.*, 2008, 2115–2117.

33 C. Li, Y. Liu, Y. Wu, Y. Sun and F. Li, *Biomaterials*, 2013, **34**, 1223–1234.

34 P. K. Lee, W. H. Law, H. W. Liu and K. K. Lo, *Inorg. Chem.*, 2011, **50**, 8570–8579.

35 R. Guan, Y. Chen, L. Zeng, T. W. Rees, C. Jin, J. Huang, Z. S. Chen, L. Ji and H. Chao, *Chem. Sci.*, 2018, **9**, 5183–5190.

36 J. J. Cao, Y. Zheng, X. W. Wu, C. P. Tan, M. H. Chen, N. Wu, L. N. Ji and Z. W. Mao, *J. Med. Chem.*, 2019, **62**, 3311–3322.

37 P. Y. Zhang, C. K. C. Chiu, H. Y. Huang, Y. P. Y. Lam, A. Habtemariam, T. Malcomson, M. J. Paterson, G. J. Clarkson, P. B. O'Connor, H. Chao and P. J. Sadler, *Angew. Chem., Int. Ed.*, 2017, **56**, 14898–14902.

38 L. He, J. J. Cao, D. Y. Zhang, L. Hao, M. F. Zhang, C. P. Tan, L. N. Ji and Z. W. Mao, *Sens. Actuators, B*, 2018, **262**, 313–325.

39 D. Y. Zhang, Y. Zheng, H. Zhang, J. H. Sun, C. P. Tan, L. He, W. Zhang, L. N. Ji and Z. W. Mao, *Adv. Sci.*, 2018, **5**, 1800581.

40 M. P. Murphy and R. C. Hartley, *Nat. Rev. Drug Discovery*, 2018, **17**, 865–886.

41 S. Yi, Z. Lu, J. Zhang, J. Wang, Z. Xie and L. Hou, *ACS Appl. Mater. Interfaces*, 2019, **11**, 15276–15289.

42 Y. Li, C. P. Tan, W. Zhang, L. He, L. N. Ji and Z. W. Mao, *Biomaterials*, 2015, **39**, 95–104.

43 L. He, M. F. Zhang, Z. Y. Pan, K. N. Wang, Z. J. Zhao, Y. Li and Z. W. Mao, *Chem. Commun.*, 2019, **55**, 10472–10475.

44 J. J. Cao, C. P. Tan, M. H. Chen, N. Wu, D. Y. Yao, X. G. Liu, L. N. Ji and Z. W. Mao, *Chem. Sci.*, 2017, **8**, 631–640.

45 M. H. Chen, F. X. Wang, J. J. Cao, C. P. Tan, L. N. Ji and Z. W. Mao, *ACS Appl. Mater. Interfaces*, 2017, **9**, 13304–13314.

46 V. Venkatesh, R. Berrocal-Martin, C. J. Wedge, I. Romero-Canelon, C. Sanchez-Cano, J. I. Song, J. P. C. Coverdale, P. Zhang, G. J. Clarkson, A. Habtemariam, S. W. Magennis, R. J. Deeth and P. J. Sadler, *Chem. Sci.*, 2017, **8**, 8271–8278.

47 R. Bevernaegie, B. Doix, E. Bastien, A. Diman, A. Decottignies, O. Feron and B. Elias, *J. Am. Chem. Soc.*, 2019, **141**, 18486–18491.

48 H. Huang, S. Banerjee, K. Qiu, P. Zhang, O. Blacque, T. Malcomson, M. J. Paterson, G. J. Clarkson, M. Staniforth, V. G. Stavros, G. Gasser, H. Chao and P. J. Sadler, *Nat. Chem.*, 2019, **11**, 1041–1048.

49 R. E. Lawrence and R. Zoncu, *Nat. Cell Biol.*, 2019, **21**, 133–142.

50 C. G. Towers and A. Thorburn, *Cancer Discov.*, 2017, **7**, 1218–1220.

51 M. H. Chen, Y. Zheng, X. J. Cai, H. Zhang, F. X. Wang, C. P. Tan, W. H. Chen, L. N. Ji and Z. W. Mao, *Chem. Sci.*, 2019, **10**, 3315–3323.

52 F. X. Wang, M. H. Chen, Y. N. Lin, H. Zhang, C. P. Tan, L. N. Ji and Z. W. Mao, *ACS Appl. Mater. Interfaces*, 2017, **9**, 42471–42481.

53 L. K. McKenzie, I. V. Sazanovich, E. Baggaley, M. Bonneau, V. Guerchais, J. A. G. Williams, J. A. Weinstein and H. E. Bryant, *Chem.-Eur. J.*, 2017, **23**, 234–238.

54 W. Lv, Z. Zhang, K. Y. Zhang, H. Yang, S. Liu, A. Xu, S. Guo, Q. Zhao and W. Huang, *Angew. Chem., Int. Ed.*, 2016, **55**, 9947–9951.

55 S. Kuang, X. Liao, X. Zhang, T. W. Rees, R. Guan, K. Xiong, Y. Chen, L. Ji and H. Chao, *Angew. Chem., Int. Ed.*, 2020, **59**, 3315–3321.

56 T. L. Lam, K. C. Tong, C. Yang, W. L. Kwong, X. Guan, M. D. Li, V. Kar-Yan Lo, S. Lai-Fung Chan, D. Lee Phillips, C. N. Lok and C. M. Che, *Chem. Sci.*, 2019, **10**, 293–309.

57 P. Zhang, H. Huang, S. Banerjee, G. J. Clarkson, C. Ge, C. Imberti and P. J. Sadler, *Angew. Chem., Int. Ed.*, 2019, **58**, 2350–2354.

58 S. A. McFarland, A. Mandel, R. Dumoulin-White and G. Gasser, *Curr. Opin. Chem. Biol.*, 2020, **56**, 23–27.

59 J. Shum, P. K. Leung and K. K. Lo, *Inorg. Chem.*, 2019, **58**, 2231–2247.

60 K. E. Erkkila, D. T. Odom and J. K. Barton, *Chem. Rev.*, 1999, **99**, 2777–2795.

61 R. E. Holmlin, E. D. Stemp and J. K. Barton, *Inorg. Chem.*, 1998, **37**, 29–34.

62 C. A. Puckett and J. K. Barton, *J. Am. Chem. Soc.*, 2007, **129**, 46–47.



63 G. Di Marco, M. Lanza and S. Campagna, *Adv. Mater.*, 1995, **7**, 468–471.

64 A. Byrne, C. S. Burke and T. E. Keyes, *Chem. Sci.*, 2016, **7**, 6551–6562.

65 S. Sreedharan, M. R. Gill, E. Garcia, H. K. Saeed, D. Robinson, A. Byrne, A. Cadby, T. E. Keyes, C. Smythe, P. Pellett, J. B. de la Serna and J. A. Thomas, *J. Am. Chem. Soc.*, 2017, **139**, 15907–15913.

66 Z. N. Zhao, P. Gao, Y. Y. You and T. F. Chen, *Chem.-Eur. J.*, 2018, **24**, 3289–3298.

67 J. Li, L. L. Zeng, K. Xiong, T. W. Rees, C. Z. Jin, W. J. Wu, Y. Chen, L. N. Ji and H. Chao, *Chem. Commun.*, 2019, **55**, 10972–10975.

68 Z. Zhao, X. Zhang, C. E. Li and T. Chen, *Biomaterials*, 2019, **192**, 579–589.

69 J. P. Liu, Y. Chen, G. Y. Li, P. Y. Zhang, C. Z. Jin, L. L. Zeng, L. N. Ji and H. Chao, *Biomaterials*, 2015, **56**, 140–153.

70 C. S. Burke, A. Byrne and T. E. Keyes, *Angew. Chem., Int. Ed.*, 2018, **57**, 12420–12424.

71 H. Y. Huang, B. L. Yu, P. Y. Zhang, J. J. Huang, Y. Chen, G. Gasser, L. N. Ji and H. Chao, *Angew. Chem., Int. Ed.*, 2015, **54**, 14049–14052.

72 H. K. Saeed, P. J. Jarman, S. Archer, S. Sreedharan, I. Q. Saeed, L. K. Mckenzie, J. A. Weinstein, N. J. Buurma, C. G. W. Smythe and J. A. Thomas, *Angew. Chem., Int. Ed.*, 2017, **56**, 12628–12633.

73 Z. X. Zhou, J. P. Liu, T. W. Rees, H. Wang, X. P. Li, H. Chao and P. J. Stang, *Proc. Natl. Acad. Sci. U. S. A.*, 2018, **115**, 5664–5669.

74 J. Yang, J. X. Zhao, Q. Cao, L. Hao, D. Zhou, Z. Gan, L. N. Ji and Z. W. Mao, *ACS Appl. Mater. Interfaces*, 2017, **9**, 13900–13912.

75 A. M. Yip, J. Shum, H. W. Liu, H. Zhou, M. Jia, N. Niu, Y. Li, C. Yu and K. K. Lo, *Chem.-Eur. J.*, 2019, **25**, 8970–8974.

76 M. W. Louie, T. T. Fong and K. K. Lo, *Inorg. Chem.*, 2011, **50**, 9465–9471.

77 K. K. Lo, M. W. Louie, K. S. Sze and J. S. Lau, *Inorg. Chem.*, 2008, **47**, 602–611.

78 A. W. Choi, K. K. Tso, V. M. Yim, H. W. Liu and K. K. Lo, *Chem. Commun.*, 2015, **51**, 3442–3445.

79 B. Albada and N. Metzler-Nolte, *Chem. Rev.*, 2016, **116**, 11797–11839.

80 I. Kitanovic, S. Z. Can, H. Alborzinia, A. Kitanovic, V. Pierroz, A. Leonidova, A. Pinto, B. Spingler, S. Ferrari, R. Molteni, A. Steffen, N. Metzler-Nolte, S. Wolf and G. Gasser, *Chem.-Eur. J.*, 2014, **20**, 2496–2507.

81 K. M. Knopf, B. L. Murphy, S. N. MacMillan, J. M. Baskin, M. P. Barr, E. Boros and J. J. Wilson, *J. Am. Chem. Soc.*, 2017, **139**, 14302–14314.

82 I. Chakraborty, J. Jimenez, W. M. C. Sameera, M. Kato and P. K. Mascharak, *Inorg. Chem.*, 2017, **56**, 2863–2873.

83 S. Imstepf, V. Pierroz, R. Rubbiani, M. Felber, T. Fox, G. Gasser and R. Alberto, *Angew. Chem., Int. Ed.*, 2016, **55**, 2792–2795.

84 C. C. Konkankit, A. P. King, K. M. Knopf, T. L. Southard and J. J. Wilson, *ACS Med. Chem. Lett.*, 2019, **10**, 822–827.

85 S. C. Marker, A. P. King, R. V. Swanda, B. Vaughn, E. Boros, S. B. Qian and J. J. Wilson, *Angew. Chem., Int. Ed.*, 2020, **59**, 13391–13400.

86 C. C. Konkankit, J. Lovett, H. H. Harris and J. J. Wilson, *Chem. Commun.*, 2020, **56**, 6515–6518.

87 A. P. King, S. C. Marker, R. V. Swanda, J. J. Woods, S. B. Qian and J. J. Wilson, *Chem.-Eur. J.*, 2019, **25**, 9206–9210.

88 J. Yang, Q. Cao, H. Zhang, L. Hao, D. Zhou, Z. Gan, Z. Li, Y. X. Tong, L. N. Ji and Z. W. Mao, *Biomaterials*, 2018, **176**, 94–105.

89 F. X. Wang, J. H. Liang, H. Zhang, Z. H. Wang, Q. Wan, C. P. Tan, L. N. Ji and Z. W. Mao, *ACS Appl. Mater. Interfaces*, 2019, **11**, 13123–13133.

90 Z. Y. Pan, C. P. Tan, L. S. Rao, H. Zhang, Y. Zheng, L. Hao, L. N. Ji and Z. W. Mao, *Angew. Chem., Int. Ed.*, 2020, **59**, 18755–18762.

